

# THEORETICAL SOLUTIONS FOR LOW-PÉCLÉT-NUMBER THERMAL-ENTRY-REGION HEAT TRANSFER IN LAMINAR FLOW THROUGH CONCENTRIC ANNULI\*

CHIA-JUNG HSU

Brookhaven National Laboratory, Upton, New York 11973, U.S.A.

(Received 20 January 1970 and in revised form 31 March 1970)

**Abstract**—Exact temperature solutions and theoretical Nusselt curves, valid for Péclet numbers ranging from 1 to  $\infty$ , were obtained for thermal-entry-region heat transfer for laminar flow through concentric annuli, subject to a step jump in wall heat flux at  $z = 0$ . To allow for the effect of axial conduction, which is significant at low Péclet numbers, the inlet fluid temperature was taken to be uniform at  $z = -\infty$ , and the first twenty eigenconstants were computed for the adiabatic region ( $-\infty < z \leq 0$ ) and the heated region ( $0 \leq z < \infty$ ), separately. By constructing two sets of orthonormal functions from the non-orthogonal eigenfunctions, the series expansion coefficients were then determined such that both the temperatures and longitudinal temperature gradients for the two regions match at  $z = 0$ . The temperature solutions corresponding to the limiting case of  $N_{Pe} = \infty$  show excellent agreement with those reported by Lundberg *et al.* [4], who analyzed the entry-region problem by neglecting axial conduction.

## NOMENCLATURE

$[B_n]_j$	series expansion coefficients in equation (16);
$C_0$ ,	a constant;
$C_1$ ,	a constant given by equation (10);
$C_2$ ,	a constant given by equation (12);
$[C_n]_j$	series expansion coefficients in equation (17);
$C_p$ ,	specific heat;
$D_h$ ,	$= 2(r_2 - r_1)$ , hydraulic diameter;
$[E]_j$ , $[F]_j$ , $[G]_j$	matrices;
$K$ ,	$= (\sigma^2 - 1)/\ln \sigma$ ;
$N_{Pe}$ ,	$= D_h \bar{u} \rho C_p / k$ , Péclet number;
$[Nu]_1$ ,	local Nusselt number defined by equation (41), for the case where step jump in heat flux occurs at the inner wall of an annulus;
$[Nu]_2$ ,	local Nusselt number defined by equation (42) for the case where step jump in heat flux occurs at the outer wall of an annulus;
$R_n(\xi)$ ,	eigenfunctions for equations (20) and (21);
$R_n(1)$ ,	$R_n(\xi)$ evaluated at $\xi = 1$ ;
$T_0$ ,	inlet fluid temperature;
$[T_i]_j$	fluid temperature in the adiabatic region ( $i = 1$ ), and in the heated region ( $i = 2$ );
$[T_f]_j$	fluid temperature in the fully developed region;
$[T_2]_j$	bulk fluid temperature in the heated region;
$[T_w]_j$	wall temperature in the heated region;

\* This work was performed under the auspices of the U.S. Atomic Energy Commission.

$Y_n(\xi)$ ,	eigenfunctions of equations (18) and (19);
$a_n^k, b_n^k$ ,	coefficients in equation (24);
$p_n^k, q_n^k$ ,	coefficients in equation (27);
$q_w$ ,	uniform heat flux at wall;
$r$ ,	radial coordinate variable;
$r_1, r_2$ ,	the inner and outer radius respectively of an annulus;
$\bar{u}$ ,	average fluid velocity;
$z$ ,	axial coordinate variable;
$\alpha_n$ ,	eigenvalues of equations (18) and (19);
$\beta_n$ ,	eigenvalues of equations (20) and (21);
$\Delta_n$ ,	Gramm determinant;
$\delta_{ij}$ ,	Kronecker delta;
$\eta$ ,	$= z/D_h N_{Pe}$ ;
$[\Theta_2]_j$ ,	$= [\theta_2]_j - [\theta_f]_j$ ;
$[\theta_i]_j$ ,	$= k\{[T_i]_j - T_0\}/q_w D_h$ , dimensionless fluid temperature;
$[\bar{\theta}_i]_j$ ,	dimensionless bulk fluid temperature;
$[\theta_f]_j$ ,	dimensionless fluid temperature in the fully developed region;
$[\bar{\theta}_f]_j$ ,	dimensionless bulk fluid temperature in the fully developed region;
$\theta_\eta$ ,	dimensionless fluid temperature at a location $\eta$ ;
$\bar{\theta}_\eta$ ,	dimensionless bulk fluid temperature at a location $\eta$ ;
$[\theta_w]_j$ ,	dimensionless wall temperature;
$\xi$ ,	$= r/r_2$ ;
$\rho$ ,	density of fluid;
$\sigma$ ,	$= r_1/r_2$ ;
$\phi(\sigma)$ ,	$= 1 + \sigma^2 - K$ ;
$\phi_k$ ,	orthonormal set of functions defined by equation (24);
$\psi$ ,	a function defined by equation (3);
$\psi_k$ ,	orthonormal set of functions defined by equation (24).

## INTRODUCTION

THE RELATIVE importance of axial conduction in heat transfer to a fluid flowing inside a channel depends primarily on the magnitude of the Péclet number. For laminar flow through a circular pipe, for instance, axial conduction is virtually negligible in comparison with radial conduction if Péclet number,  $N_{Pe}$ , exceeds approximately 100. The classic Graetz problem deals with thermal-entry-region heat transfer under such a condition. For  $N_{Pe} < 100$ , however, axial conduction becomes increasingly important as  $N_{Pe}$  is reduced. It ultimately attains an order of magnitude equal to that of radial conduction as  $N_{Pe}$  approaches unity. For a thorough understanding of the heat transfer characteristics, explicit temperature solutions, valid for such small Péclet numbers, are of great theoretical value. Mathematically speaking, however, such solutions are much more difficult to seek than those for the Graetz-type problem, because not only does the energy equation contain an additional axial conduction term, but that the heat transfer needs to be considered in the infinite region,  $-\infty < z < \infty$ , rather than the semi-infinite region,  $0 \leq z < \infty$ . The latter requirement arises from the fact that the thermal effect of axial conduction, under ordinary circumstances, penetrates into the region  $0 > z$ , thus enlarging the domain of heat transfer. In practice, therefore, it is no longer realistic to specify the inlet fluid temperature at  $z = 0$ . Instead, such a boundary condition should be imposed at  $z = -\infty$ .

A mathematical scheme for solving this type of convection heat transfer problem in the infinite region,  $-\infty < z < \infty$ , was recently devised by the present author [2]. The method consists essentially of determining the eigenvalues and eigenfunctions for the regions  $z \leq 0$  and  $z \geq 0$ , separately, and then matching both the temperatures and longitudinal temperature gradients at  $z = 0$ . To accomplish the matching process, two orthonormal sets of functions were constructed from the nonorthogonal eigenfunctions by utilizing the Gramm-Schmidt orthonormalization procedure [3], and the series expansion coefficients were then determined by solving a system of simultaneous equations. For laminar flow inside a circular pipe with a step change in wall heat flux at  $z = 0$ , the proposed scheme was shown [2] to yield Nusselt numbers that agree almost perfectly with those reported recently by Hennecke [1], who solved the same set of partial differential equations numerically using the finite-difference approach. It was also demonstrated that the theoretical solution obtained by the proposed method, in fact, represents a more generalized thermal-entry-region temperature solution, which reduces to that for the corresponding Graetz problem as  $N_{pe}$  approaches infinity.

The objective of the present study was to apply the same technique to analyze the corresponding problem for laminar flow through concentric annuli, for which no solutions, numerical or theoretical, have hitherto been reported in the literature. Theoretical solutions are presented in this paper for unilateral heat transfer from either the inner or outer wall of an annulus subject to a step change in wall heat flux at  $z = 0$ . The opposite wall, in either case, was considered thermally adiabatic. Nusselt curves were obtained for Péclet numbers ranging from 1 to  $\infty$ , for annuli having the inner-to-outer radius ratio ( $r_1/r_2$ ) of 0.1, 0.3, 0.5, 0.7 and 0.9. As will be shown later, the Nusselt numbers corresponding to  $N_{pe} = \infty$  agree very well with those obtained by Lundberg *et al.* [4], who analyzed the corresponding problem by assuming negligible axial conduction. From the explicit temperature solutions, the local temperature profiles in both the adiabatic and heated regions were also calculated and illustrated.

### THEORETICAL ANALYSIS

A schematic diagram is shown in Fig. 1 for laminar incompressible flow through an annulus having an adiabatic inner wall and an outer wall that is subjected to a step change in heat flux at  $z = 0$ . In the analysis that follows, the temperature solutions corresponding to this case will be discerned by a subscript,  $j = 2$ . By interchanging the thermal boundary conditions at the inner and outer walls, one obtains the diagram for the case in which the step change in heat flux is imposed at the inner

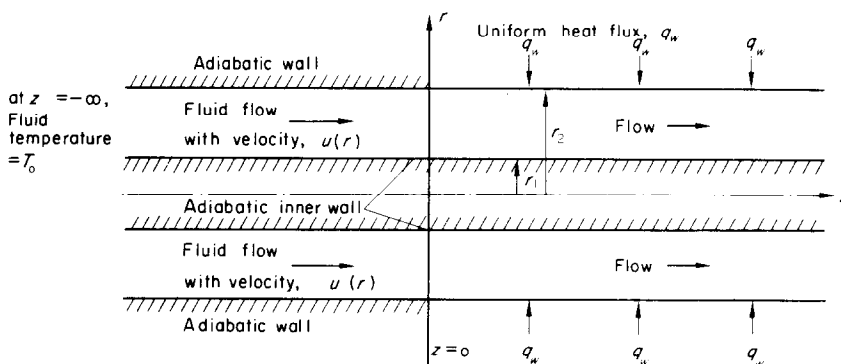


FIG. 1. Coordinate system for the annular channel.

wall. The temperature solutions for this latter case will be denoted by a subscript,  $j = 1$ . In either case, the inlet fluid temperature is uniform and equals  $T_0$  at  $z = -\infty$ . The energy equations, by assuming constant fluid properties and negligible viscous dissipation, can then be written for  $j = 1$  or 2, as

$$2\rho\bar{u}C_p \left[ \frac{1 - (r/r_2)^2 + \left(\frac{\sigma^2 - 1}{\ln \sigma}\right) \ln(r/r_2)}{1 + \sigma^2 - \left(\frac{\sigma^2 - 1}{\ln \sigma}\right)} \right] \frac{\partial [T_i]_j}{\partial z} = k \left[ \frac{\partial^2 [T_i]_j}{\partial r^2} + \frac{1}{r} \frac{\partial [T_i]_j}{\partial r} + \frac{\partial^2 [T_i]_j}{\partial z^2} \right] \quad (i = 1, 2), \quad (1)$$

where the subscript "i" in  $[T_i]_j$  ( $i = 1$  and  $i = 2$ ) refers to the adiabatic region ( $-\infty < z \leq 0$ ) and the heated region ( $0 \leq z < \infty$ ) respectively. The appropriate boundary conditions to be satisfied are:

For the region  $-\infty < z \leq 0$ , and for  $j = 1$  or 2,

$$[T_1]_j = T_0 \quad \text{at } z = -\infty \quad (2.1)$$

$$\frac{\partial [T_1]_j}{\partial r} = 0 \quad \text{at } r = r_1 \text{ and } r = r_2. \quad (2.2)$$

For the region  $0 \leq z < \infty$ , and for  $j = 1$  or 2,

$$[T_2]_j = [T_j]_j \quad \text{as } z \rightarrow \infty \quad (2.3)$$

$$\frac{\partial [T_2]_j}{\partial r} = -\delta_{1j}(q_w/k) \quad \text{at } r = r_1 \quad (2.4)$$

$$\frac{\partial [T_2]_j}{\partial r} = \delta_{2j}(q_w/k) \quad \text{at } r = r_2 \quad (2.5)$$

where  $\delta_{kj}$  ( $k = 1, 2$ ) is the Kronecker delta, i.e.

$$\delta_{kj} = \begin{cases} 1 & \text{if } k = j \\ 0 & \text{if } k \neq j \end{cases}$$

At  $z = 0$ , and for  $j = 1$  or 2,

$$[T_1]_j(r) = [T_2]_j(r), \quad \frac{\partial [T_1]_j(r)}{\partial z} = \frac{\partial [T_2]_j(r)}{\partial z}. \quad (2.6)$$

For each value of  $j$  (i.e.  $j = 1$  or 2), equation (1) represents a set of elliptic partial differential equations. Their solutions satisfying the boundary conditions (2.1)–(2.5) are to be matched at  $z = 0$  such that the two conditions given by equation (2.6) are both satisfied. To seek the mathematical solutions to equations (1)–(2.6), it is advantageous to change the variables by letting  $[\theta_i]_j = k([T_i]_j - T_0)/q_w D_n$ ,  $\eta = z/D_n N_{Pe}$ ,  $\xi = r/r_2$ ,  $K = (\sigma^2 - 1)/\ln \sigma$  and  $\phi(\sigma) = 1 + \sigma^2 - K$ . The above set of equations are then transformed, for  $j = 1$  or 2, to:

$$\frac{1 - \xi^2 + K \ln \xi}{2\phi(\sigma)(1 - \sigma)^2} \frac{\partial [\theta_i]_j}{\partial \eta} = \frac{\partial^2 [\theta_i]_j}{\partial \xi^2} + \frac{1}{\xi} \frac{\partial [\theta_i]_j}{\partial \xi} + \frac{1}{4(1 - \sigma)^2 N_{Pe}^2} \frac{\partial^2 [\theta_i]_j}{\partial \eta^2} \quad (i = 1, 2). \quad (1')$$

For the region  $-\infty < \eta \leq 0$ , and for  $j = 1$  or  $2$ ,

$$[\theta_1]_j = 0 \quad \text{at } \eta = -\infty \tag{2.1}'$$

$$\frac{\partial[\theta_1]_j}{\partial \xi} = 0 \quad \text{at } \xi = \sigma \text{ and } \xi = 1. \tag{2.2}'$$

For the region  $0 \leq \eta < \infty$ , and for  $j = 1$  or  $2$ ,

$$[\theta_2]_j = [\theta_f]_j \quad \text{as } \eta \rightarrow \infty \tag{2.3}'$$

$$\frac{\partial[\theta_2]_j}{\partial \xi} = -\delta_{1j}/2(1 - \sigma) \quad \text{at } \xi = \sigma \tag{2.4}'$$

$$\frac{\partial[\theta_2]_j}{\partial \xi} = \delta_{2j}/2(1 - \sigma) \quad \text{at } \xi = 1. \tag{2.5}'$$

At  $\eta = 0$ , and for  $j = 1$  or  $2$ ,

$$[\theta_1]_j(\xi) = [\theta_2]_j(\xi), \quad \frac{\partial[\theta_1]_j(\xi)}{\partial \eta} = \frac{\partial[\theta_2]_j(\xi)}{\partial \eta}. \tag{2.6}'$$

In equation (2.3)',  $[\theta_f]_j$  ( $j = 1$  or  $2$ ) denotes the dimensionless, fully developed temperature solution which includes the effect of upstream conduction. It can be derived in the following manner. To seek the expression for  $[\theta_f]_1$ , for example, a solution of the form:

$$[\theta_f]_1 = C_0 \eta + \psi(\xi) \tag{3}$$

is assumed on the fact that, in the thermally fully developed region, the temperature solution is a linear function of  $\eta$ . Substituting equation (3) into equations (1)', (2.4)' and (2.5)' then yields the following ordinary differential equation and the boundary conditions.

$$\frac{d^2 \psi}{d\xi^2} + \frac{1}{\xi} \frac{d\psi}{d\xi} = C_0 \left[ \frac{1 - \xi^2 + K \ln \xi}{2\phi(\sigma)(1 - \sigma)^2} \right] \tag{4}$$

$$\frac{d\psi}{d\xi} = \frac{-1}{2(1 - \sigma)} \quad \text{at } \xi = \sigma \tag{5}$$

$$\frac{d\psi}{d\xi} = 0 \quad \text{at } \xi = 1. \tag{6}$$

Integrating equation (4) twice, applying the boundary conditions, and then combining the results with equation (3) gives:

$$[\theta_f]_1 = \left( \frac{4\sigma}{1 + \sigma} \right) \eta + \frac{\sigma}{\phi(\sigma)(1 + \sigma)(1 - \sigma)^2} \left[ \frac{(1 - K)}{2} (\xi^2 - \ln \xi) - \frac{\xi^4}{8} + \frac{K\xi^2}{2} \ln \xi \right] + C1. \tag{7}$$

To evaluate the integration constant, C1, in equation (7), a heat balance over the region extending from  $z = -\infty$  to an arbitrary position in the thermally fully developed region is taken. Denoting the dimensionless bulk fluid temperature at the latter position by  $[\bar{\theta}]_1$ , one obtains:

$$[\bar{\theta}]_1 = \frac{4\sigma}{1 + \sigma} \eta + \frac{2}{(1 - \sigma^2) N_{pe}^2} \int_{\sigma}^1 \xi \frac{\partial[\theta_f]_1}{\partial \eta} d\xi = \frac{4\sigma}{1 + \sigma} \left[ \eta + \frac{1}{N_{pe}^2} \right]. \tag{8}$$

Since the bulk fluid temperature at any axial position,  $\eta$ , is given by the general expression

$$\bar{\theta}_\eta = \frac{4}{\phi(\sigma)(1 - \sigma^2)} \int_\sigma^1 \xi(1 - \xi^2 + K \ln \xi) \theta_\eta d\xi, \tag{9}$$

substitution of equation (7) into equation (9), followed by an integration and comparison with equation (8), gives, after considerable algebraic manipulation, the following expression for C1.

$$C1 = \frac{-\sigma}{\phi^2(\sigma)(1 + \sigma)(1 - \sigma)^2} \left[ \left( \frac{25}{48} - \frac{11}{9} K + \frac{11}{16} K^2 \right) + \left( \frac{49}{48} - \frac{11}{9} K + \frac{3}{16} K^2 \right) \sigma^2 \right. \\ \left. + \left( \frac{31}{48} - \frac{25}{72} K - \frac{1}{2K} \right) \sigma^4 + \frac{7}{48} \sigma^6 \right] + \frac{4\sigma}{1 + \sigma} \frac{1}{N_{Pe}^2}. \tag{10}$$

Combining equations (10) and (7) yields the expression for  $[\theta_f]_1$ , which differs from that for the case of no axial conduction in that it contains an additional term,  $4\sigma/(1 + \sigma) N_{Pe}^2$ . By proceeding in the same manner,  $[\theta_f]_2$  can be found to be:

$$[\theta_f]_2 = \frac{4\eta}{1 + \sigma} + \frac{1}{\phi(\sigma)(1 + \sigma)(1 - \sigma)^2} \left[ \left( \frac{1 - K}{2} \right) \xi^2 - \frac{\xi^4}{8} + \frac{K\xi^2 \ln \xi}{2} - \frac{\sigma^2}{2} (\sigma^2 - K) \ln \xi \right] + C2 \tag{11}$$

where

$$C2 = \frac{-1}{\phi^2(\sigma)(1 + \sigma)(1 - \sigma)^2} \left[ \left( \frac{7}{48} - \frac{25}{72} K + \frac{3}{16} K^2 \right) + \left( \frac{7}{48} - \frac{13}{18} K + \frac{11}{16} K^2 \right) \sigma^2 \right. \\ \left. + \left( \frac{25}{48} - \frac{31}{18} K \right) \sigma^4 + \frac{73}{48} \sigma^6 - \frac{\sigma^8}{2K} \right] + \frac{4}{1 + \sigma} \frac{1}{N_{Pe}^2}. \tag{12}$$

The boundary condition, equation (2.3), is now completely specified. To solve equations (1)-(2.6), for  $[\theta_2]_j$ , it is further convenient to let

$$[\theta_2]_j = [\Theta_2]_j + [\theta_f]_j \quad (j = 1 \text{ or } 2) \tag{13}$$

from which one can readily conclude that  $[\Theta_2]_j$  needs to satisfy the following partial differential equation and the boundary conditions.

$$\left[ \frac{1 - \xi^2 + K \ln \xi}{2\phi(\sigma)(1 - \sigma)^2} \right] \frac{\partial [\Theta_2]_j}{\partial \eta} = \frac{\partial^2 [\Theta_2]_j}{\partial \xi^2} + \frac{1}{\xi} \frac{\partial [\Theta_2]_j}{\partial \xi} + \frac{1}{4(1 - \sigma)^2 N_{Pe}^2} \frac{\partial^2 [\Theta_2]_j}{\partial \eta^2} \tag{14}$$

$$[\Theta_2]_j \rightarrow 0 \quad \text{as } \eta \rightarrow \infty \tag{15.1}$$

$$\frac{\partial [\Theta_2]_j}{\partial \xi} = 0 \quad \text{at } \xi = \sigma \text{ and } \xi = 1. \tag{15.2}$$

The temperature solutions,  $[\theta_1]_j$  and  $[\Theta_2]_j$ , are now sought in the form:

$$[\theta_1]_j = \sum_{n=1}^{\infty} [B_n]_j Y_n(\xi) \exp [\alpha_n^2 \eta] \tag{16}$$

$$[\Theta_2]_j = \sum_{n=1}^{\infty} [C_n]_j R_n(\xi) \exp [-\beta_n^2 \eta] \tag{17}$$

(j = 1 or 2)

which satisfies respectively equation (2.1)' and equation (15.1). In equation (16),  $\alpha_n$  and  $Y_n(\xi)$  are the eigenvalues and the corresponding eigenfunctions of the following characteristic equation and the boundary conditions.

$$\frac{d^2 Y_n}{d\xi^2} + \frac{1}{\xi} \frac{dY_n}{d\xi} + \alpha_n^2 \left[ \frac{\alpha_n^2}{4(1-\sigma)^2 N_{pe}^2} - \frac{(1-\xi^2) + K \ln \xi}{2\phi(\sigma)(1-\sigma)^2} \right] Y_n = 0 \tag{18}$$

$$\frac{dY_n}{d\xi} = 0 \quad \text{at } \xi = \sigma \text{ and } \xi = 1. \tag{19}$$

Similarly,  $\beta_n$  and  $R_n(\xi)$  in equation (17) represent the eigenconstants for the following characteristic equation and the boundary conditions.

$$\frac{d^2 R_n}{d\xi^2} + \frac{1}{\xi} \frac{dR_n}{d\xi} + \beta_n^2 \left[ \frac{\beta_n^2}{4(1-\sigma)^2 N_{pe}^2} + \frac{(1-\xi^2) + K \ln \xi}{2\phi(\sigma)(1-\sigma)^2} \right] R_n = 0 \tag{20}$$

$$\frac{dR_n}{d\xi} = 0 \quad \text{at } \xi = \sigma \text{ and } \xi = 1. \tag{21}$$

It is noteworthy that the negative eigenvalues of the former set of characteristic equations, i.e. equations (18) and (19), actually correspond to the positive eigenvalues of the latter set of characteristic equations, equations (20) and (21), and vice versa. The two sets of characteristic equations are, hence, intrinsically equivalent. The first twenty eigenvalues and the corresponding eigenfunctions were determined, in this study, for annuli having  $\sigma (= r_1/r_2)$  values of 0.1, 0.3, 0.5, 0.7 and 0.9 and for  $N_{pe}$  ranging from 1 to  $\infty$ . For  $N_{pe} < 100$ , the eigenvalues show a tendency to become progressively smaller as  $N_{pe}$  decreases. The eigenvalues are, however, quite insensitive to the variation of  $N_{pe}$ , if  $N_{pe}$  exceeds  $\sim 100$ . For reference, the computed eigenconstants are tabulated in Table 1 for  $N_{pe} = 1$  and  $\sigma = 0.5$ . For a pair of fixed  $N_{pe}$  and  $\sigma$ , the eigenconstants applicable to

Table 1. Calculated eigenvalues and the related constants  
 $\sigma = r_1/r_2 = 0.5, N_{pe} = 1$

$n$	$\alpha_n$	$\beta_n$	$[B_n]_1$	$[C_n]_1$	$[B_n]_2$	$[C_n]_2$	$\int_{\sigma}^1 \xi R_n d\xi$
1	0.999310	2.45771	1.33723	-4.75116(2)*	2.68973	6.95267(2)*	-3.17070(3)*
2	2.60096	3.48921	4.58435(2)*	-1.30812(2)	-6.38521(2)*	-1.86367(2)	6.90435(3)
3	3.61979	4.29095	1.16212(2)	-5.83076(3)	1.64379(2)	8.26988(3)	-1.43243(4)
4	4.40267	4.96743	5.30962(3)	-3.26591(3)	-7.51051(3)	-4.62423(3)	9.52163(4)
5	5.06580	5.56306	3.03117(3)	-2.08096(3)	4.28766(3)	2.94565(3)	-2.80348(5)
6	5.65172	6.10114	1.95805(3)	-1.44055(3)	-2.76799(3)	-2.03732(3)	2.82183(4)
7	6.18242	6.59564	1.36785(3)	-1.05523(3)	1.93389(3)	1.49292(3)	-9.87856(6)
8	6.67108	7.05565	1.00968(3)	-8.06559(4)	-1.42624(3)	-1.13979(3)	1.18508(4)
9	7.12634	7.48752	7.75420(4)	-6.35905(4)	1.09559(3)	8.99402(4)	-4.57786(6)
10	7.55424	7.89583	6.14608(4)	-5.14785(4)	-8.67198(4)	-7.26735(4)	6.04050(5)
11	7.95918	8.28407	4.98747(4)	-4.24634(4)	7.03975(4)	6.00431(4)	-2.45171(6)
12	8.34451	8.65493	4.13318(4)	-3.56990(4)	-5.82077(4)	-5.03133(4)	3.48369(5)
13	8.71282	9.01055	3.47715(4)	-3.03523(4)	4.89937(4)	4.29116(4)	-1.46014(6)
14	9.06619	9.35267	2.97220(4)	-2.62247(4)	-4.17080(4)	-3.68444(4)	2.18979(5)
15	9.40630	9.68272	2.56501(4)	-2.27659(4)	3.60175(4)	3.22068(4)	-9.478468(7)
16	9.73455	10.00190	2.24590(4)	-2.01059(4)	-3.12620(4)	-2.80511(4)	1.48519(5)
17	10.05209	10.31121	1.97593(4)	-1.76550(4)	2.75214(4)	2.51441(4)	-9.22116(7)
18	10.35990	10.61151	1.77306(4)	-1.57387(4)	-2.40577(4)	-2.15488(4)	1.01823(5)
19	10.65884	10.90356	1.58699(4)	-1.25311(4)	2.14973(4)	2.19246(4)	-5.61137(7)
20	10.94963	11.18799	1.60089(4)	-2.95197(4)	-1.67277(4)	-3.10362(4)	7.28163(6)

\*  $X(a)$  means  $X \times 10^{-a}$ .

equations (16) and (17) do not depend upon whether the step jump in heat flux occurs at the inner or outer wall of an annulus. The series expansion coefficients,  $[B_n]_j$  and  $[C_n]_j$ , however, are contingent upon such boundary conditions. From equation (2.6), it is apparent that these coefficients must be determined such that the following two equations are simultaneously satisfied.

$$\sum_{n=1}^{\infty} [C_n]_j R_n(\xi) - \sum_{n=1}^{\infty} [B_n]_j Y_n(\xi) = -[\theta_f]_{j, n=0} \tag{22}$$

$$\sum_{n=1}^{\infty} \beta_n^2 [C_n]_j R_n(\xi) + \sum_{n=1}^{\infty} \alpha_n^2 [B_n]_j Y_n(\xi) = \frac{4}{1 + \sigma} [\delta_{1j}\sigma + \delta_{2j}]. \tag{23}$$

Neither  $R_n(\xi)$  nor  $Y_n(\xi)$  constitutes a set of mutually orthogonal functions, as is clear from the form of equations (18)–(21). The eigenfunction expansion technique customarily employed for the differential equations of the Sturm–Liouville system, therefore, cannot be utilized to evaluate the series expansion coefficients. As was done in the previous study [2], therefore, two sets of orthonormal functions,  $\psi_k$  and  $\phi_k$ , were constructed by linearly combining  $R_n$  or  $Y_n$  such that,

$$\psi_k = \sum_{n=1}^k a_n^k R_n(\xi), \quad \phi_k = \sum_{n=1}^k b_n^k Y_n(\xi), \quad k = 1, 2, \dots \tag{24}$$

and having the properties,

$$\int_{\sigma}^1 \psi_i \psi_k d\xi = \begin{cases} 0 & \text{if } i \neq k \\ 1 & \text{if } i = k \end{cases}, \quad \int_{\sigma}^1 \phi_i \phi_k d\xi = \begin{cases} 0 & \text{if } i \neq k \\ 1 & \text{if } i = k \end{cases}. \tag{25}$$

Construction of such orthonormal sets of function is possible by virtue of the fact that each of the eigenfunctions,  $R_n$  or  $Y_n$  ( $n = 1, 2, 3, \dots$ ), constitutes a set of linearly independent vectors. The orthonormalization can be performed step by step following the Gram–Schmidt orthonormalization procedure [3]. For example,

$$\psi_1 = R_1(\xi)/(\sqrt{\Delta_1}), \quad \psi_2 = \left| \begin{array}{c} \int_{\sigma}^1 R_1^2 d\xi R_1 \\ \int_{\sigma}^1 R_2 R_1 d\xi R_2 \end{array} \right| \sqrt{(\Delta_1 \Delta_2)}, \text{ etc.,}$$

and in general,

$$\psi_n = \frac{\begin{vmatrix} \int_{\sigma}^1 R_1^2 d\xi & \int_{\sigma}^1 R_2 R_1 d\xi & \dots & \int_{\sigma}^1 R_1 R_{n-1} d\xi & R_1(\xi) \\ \int_{\sigma}^1 R_2 R_1 d\xi & \int_{\sigma}^1 R_2^2 d\xi & \dots & \int_{\sigma}^1 R_2 R_{n-1} d\xi & R_2(\xi) \\ \dots & \dots & \dots & \dots & \dots \\ \int_{\sigma}^1 R_n R_1 d\xi & \int_{\sigma}^1 R_n R_2 d\xi & \dots & \int_{\sigma}^1 R_n R_{n-1} d\xi & R_n(\xi) \end{vmatrix}}{\sqrt{(\Delta_n \cdot \Delta_{n-1})}} \tag{26}$$

where  $\Delta_n$  is the Gram-determinant which can be obtained by replacing the elements in the last



column of the above determinant,  $R_i(\xi)$ , ( $i = 1, 2, \dots$ ), by  $\int_{\sigma}^1 R_i R_n d\xi$  ( $i = 1, 2, \dots$ ). In this study,  $\psi_k$  and  $\phi_k$  were constructed for  $k = 1-20$ . By the following linear transformations,  $R_n$  and  $Y_n$  can be expressed conversely in terms of  $\psi_n$  and  $\phi_n$ .

$$R_k = \sum_{n=1}^k p_n^k \psi_n(\xi), \quad Y_k = \sum_{n=1}^k q_n^k \phi_n(\xi), \quad k = 1, 2, \dots \tag{27}$$

The numerical coefficients,  $p_n^k$  and  $q_n^k$ , can be obtained most conveniently by inverting the matrices containing  $a_n^k$  or  $b_n^k$  as their elements. Substitution of equation (27) into equations (22) and (23) yields, for  $j = 1$  or  $2$ ,

$$\sum_{n=1}^{\infty} \sum_{k=n}^{\infty} [C_k]_j p_n^k \psi_n(\xi) - \sum_{n=1}^{\infty} \sum_{k=n}^{\infty} [B_k]_j q_n^k \phi_n(\xi) = -[\theta_f]_{j, \eta=0} \tag{28}$$

$$\sum_{n=1}^{\infty} \sum_{k=n}^{\infty} [C_k]_j \beta_k^2 p_n^k \psi_n(\xi) + \sum_{n=1}^{\infty} \sum_{k=n}^{\infty} [B_k]_j \alpha_k^2 q_n^k \phi_n(\xi) = \frac{4}{1 + \sigma} [\delta_{1j}\sigma + \delta_{2j}] \tag{29}$$

which now permit determination of the series expansion coefficients, inasmuch as  $\psi_n(\xi)$  and  $\phi_n(\xi)$  are orthonormal sets of functions. Thus, multiplying equation (28) by  $\psi_m$ , and equation (29) by  $\phi_m$ , and integrating from  $\sigma$  to 1, the following sets of equations result by virtue of the orthonormal properties given by equation (25).

$$\sum_{k=m}^{\infty} [C_k]_j p_m^k - \sum_{n=1}^{\infty} \sum_{k=n}^{\infty} [B_k]_j q_n^k \int_{\sigma}^1 \phi_n \psi_m d\xi = - \int_{\sigma}^1 [\theta_f]_{j, \eta=0} \psi_m d\xi \tag{30}$$

$$\sum_{n=1}^{\infty} \sum_{k=n}^{\infty} [C_k]_j \beta_k^2 p_n^k \int_{\sigma}^1 \psi_n \phi_m d\xi + \sum_{k=m}^{\infty} [B_k]_j \alpha_k^2 q_m^k = \frac{4}{1 + \sigma} [\delta_{1j}\sigma + \delta_{2j}] \int_{\sigma}^1 \phi_m d\xi \quad (m = 1, 2, \dots) \tag{31}$$

The infinite series appearing in the above two equations were truncated, in this study, at  $m = 20$ , for which their solutions were found to converge satisfactorily. With  $m = 20$ , these two equations provide forty simultaneous equations which can be solved for the forty unknowns,  $[C_1]_j \sim [C_{20}]_j$  and  $[B_1]_j \sim [B_{20}]_j$ . Thus, letting

$$\begin{bmatrix} [C_1]_j \\ [C_2]_j \\ \vdots \\ [C_m]_j \\ [B_1]_j \\ [B_2]_j \\ \vdots \\ [B_m]_j \end{bmatrix} = [\vec{F}]_j = \begin{bmatrix} - \int_{\sigma}^1 [\theta_f]_{j, \eta=0} \phi_1 d\xi \\ - \int_{\sigma}^1 [\theta_f]_{j, \eta=0} \phi_2 d\xi \\ \vdots \\ \vdots \\ \frac{4}{1 + \sigma} (\delta_{1j}\sigma + \delta_{2j}) \int_{\sigma}^1 \phi_1 d\xi \\ \vdots \\ \vdots \\ \frac{4}{1 + \sigma} (\delta_{1j}\sigma + \delta_{2j}) \int_{\sigma}^1 \phi_m d\xi \end{bmatrix} = [\vec{G}]_j$$

and

$$[\vec{E}]_j = \begin{bmatrix} p_1^1 & p_1^2 & \dots & \dots & p_1^m & -q_1^1 \int_{\sigma}^1 \phi_1 \psi_1 d\xi & \dots & -\sum_{k=1}^m q_k^m \int_{\sigma}^1 \phi_k \psi_1 d\xi \\ 0 & p_2^2 & \dots & \dots & p_2^m & \dots & \dots & \dots \\ \dots & \dots & \dots & \dots & \dots & \dots & \dots & \dots \\ 0 & \dots & \dots & \dots & p_m^m & -q_1^1 \int_{\sigma}^1 \phi_1 \psi_m d\xi & \dots & -\sum_{k=1}^m q_k^m \int_{\sigma}^1 \phi_k \psi_m d\xi \\ \beta_1^2 p_1^1 \int_{\sigma}^1 \psi_1 \phi_1 d\xi & \dots & \beta_m^2 \sum_{k=1}^m p_k^m \int_{\sigma}^1 \psi_k \phi_1 d\xi & \alpha_1^2 q_1^1 & \dots & \dots & \dots & \alpha_m^2 q_1^m \\ \dots & \dots & \dots & 0 & \alpha_2^2 q_2^2 & \dots & \dots & \alpha_m^2 q_2^m \\ \dots & \dots & \dots & \dots & \dots & \dots & \dots & \dots \\ \beta_1^2 p_1^1 \int_{\sigma}^1 \psi_1 \phi_m d\xi & \dots & \beta_m^2 \sum_{k=1}^m p_k^m \int_{\sigma}^1 \psi_k \phi_m d\xi & 0 & 0 & \dots & \dots & \alpha_m^2 q_m^m \end{bmatrix}$$

the system of simultaneous equations can be written, in matrix form, as:

$$[\vec{E}]_j [\vec{F}]_j = [\vec{G}]_j \quad (j = 1 \text{ or } 2) \tag{32}$$

for which the solution can be written

$$[\vec{F}]_j = [\vec{E}^{-1}]_j [\vec{G}]_j. \tag{33}$$

The system of forty simultaneous equations was solved by utilizing the Gauss elimination method using a CDC 6600 computer. The  $[\vec{E}]_j$  matrix was normalized row-wise and reduced to a triangular form by transformations using pivotal condensations. The unknowns were then calculated by back substitutions. Whenever the computed series coefficients were found to be insufficiently accurate, a combination of the Gauss elimination method and an iteration scheme was used to improve the computational accuracy. The coefficients,  $[B_n]_j$  and  $[C_n]_j$ , thus obtained are tabulated in Table 1 for  $N_{pe} = 1$  and  $\sigma = 0.5$ .

Summing up, the solutions to equations (1)-(2.6) have been obtained as follows:

$$[\theta_1]_1 = \sum_{n=1}^{\infty} [B_n]_1 Y_n(\xi) \exp[\alpha_n^2 \eta] \tag{34}$$

$$[\theta_2]_1 = \left( \frac{4\sigma}{1+\sigma} \right) \eta + \frac{\sigma}{\phi(\sigma)(1+\sigma)(1-\sigma)^2} \left[ \left( \frac{1-K}{2} \right) (\xi^2 - \ln \xi) - \frac{\xi^4}{8} + \frac{K}{2} \xi^2 \ln \xi \right] + C1 + \sum_{n=1}^{\infty} [C_n]_1 R_n(\xi) \exp[-\beta_n^2 \eta] \tag{35}$$

$$[\theta_1]_2 = \sum_{n=1}^{\infty} [B_n]_2 Y_n(\xi) \exp[\alpha_n^2 \eta] \tag{36}$$

$$[\theta_2]_2 = \frac{4\eta}{1+\sigma} + \frac{1}{\phi(\sigma)(1+\sigma)(1-\sigma)^2} \left[ \left( \frac{1-K}{2} \right) \xi^2 - \frac{\xi^4}{8} + \frac{K\xi^2 \ln \xi}{2} - \frac{\sigma^2}{2} (\sigma^2 - K) \ln \xi \right] + C2 + \sum_{n=1}^{\infty} [C_n]_2 R_n(\xi) \exp[-\beta_n^2 \eta] \tag{37}$$

where  $C1$  and  $C2$  are given respectively by equation (10) and equation (12). Availability of the explicit temperature solutions now enables derivation of the expressions for local Nusselt numbers. Of particular interest are those in the heated region ( $0 \leq z < \infty$ ). Since the bulk fluid temperature, in dimensionless form is given by :

$$[\theta_i]_j = \frac{4}{\phi(\sigma)(1 - \sigma^2)} \int_{\sigma}^1 \xi(1 - \xi^2 + K \ln \xi) [\theta_i]_j d\xi \quad (j = 1 \text{ or } 2, i = 1, 2) \quad (38)$$

substitution of equation (35) into this equation, followed by integration, yields

$$[\theta_2]_1 = \left( \frac{4\sigma}{1 + \sigma} \right) \left( \eta + \frac{1}{N_{Pe}^2} \right) + \frac{4}{\phi(\sigma)(1 - \sigma^2)} \sum_{n=1}^{\infty} [C_n]_1 \exp[-\beta_n^2 \eta] \times \int_{\sigma}^1 (1 - \xi^2 + K \ln \xi) \xi R_n d\xi. \quad (39)$$

The integral appearing in equation (39) can be simplified to some extent by making use of equation (20). Thus, one eventually obtains

$$[\theta_2]_1 = \frac{4\sigma}{1 + \sigma} \left( \eta + \frac{1}{N_{Pe}^2} \right) - \frac{2}{(1 - \sigma^2) N_{Pe}^2} \sum_{n=1}^{\infty} [C_n]_1 \beta_n^2 \exp[-\beta_n^2 \eta] \int_{\sigma}^1 \xi R_n d\xi. \quad (40)$$

The expression for the wall temperature, meanwhile, can be found by letting  $\xi = \sigma$  in equation (35) and noting that  $R_n(\sigma)$  is arbitrarily chosen to be unity. The expression for  $[Nu]_1$  hence becomes

$$[Nu]_1 = \frac{q_w D_h}{k\{[T_w]_1 - [T_2]_1\}} = \frac{1}{[\theta_w]_1 - [\theta_2]_1} = \left\{ \frac{\sigma}{\phi(\sigma)(1 + \sigma)(1 - \sigma^2)} \left[ \left( \frac{1 - K}{2} \right) (\sigma^2 - \ln \sigma) - \frac{\sigma^4}{8} + \frac{K}{2} \sigma^2 \ln \sigma \right] + C1 + \sum_{n=1}^{\infty} [C_n]_1 \times \exp(-\beta_n^2 \eta) + \frac{2}{N_{Pe}^2(1 - \sigma^2)} \sum_{n=1}^{\infty} [C_n]_1 \beta_n^2 \exp(-\beta_n^2 \eta) \int_{\sigma}^1 \xi R_n d\xi \right\}^{-1}. \quad (41)$$

By going through an analogous derivation, the following expression for  $[Nu]_2$  can be obtained.

$$[Nu]_2 = \frac{q_w D_h}{k\{[T_w]_2 - [T_2]_2\}} = \frac{1}{[\theta_w]_2 - [\theta_2]_2} = \left[ \frac{1}{\phi(\sigma)(1 + \sigma)(1 - \sigma^2)} \left( \frac{3}{8} - \frac{K}{2} \right) + C2 + \sum_{n=1}^{\infty} [C_n]_2 R_n(1) \exp(-\beta_n^2 \eta) + \frac{2}{N_{Pe}^2(1 - \sigma^2)} \sum_{n=1}^{\infty} [C_n]_2 \beta_n^2 \exp(-\beta_n^2 \eta) \int_{\sigma}^1 \xi R_n d\xi \right]^{-1}. \quad (42)$$

It is worth remarking that, as  $N_{Pe} \rightarrow \infty$ , equations (41) and (42) each reduce to the expression for the case of negligible axial conduction.

## DISCUSSION AND CONCLUSIONS

One of the most crucial parts of this analysis, undoubtedly, is the matching of the temperatures and longitudinal temperature gradients at  $z = 0$ . To ascertain that the series expansion coefficients,  $[B_n]_j$  and  $[C_n]_j$ , computed by constructing the orthonormal functions and by solving the system of simultaneous equations indeed satisfy the required matching conditions, they were substituted into the left side of both equations (22) and (23). The results were checked with the right-hand side of these equations and it was revealed that these two equations were both satisfied remarkably well.

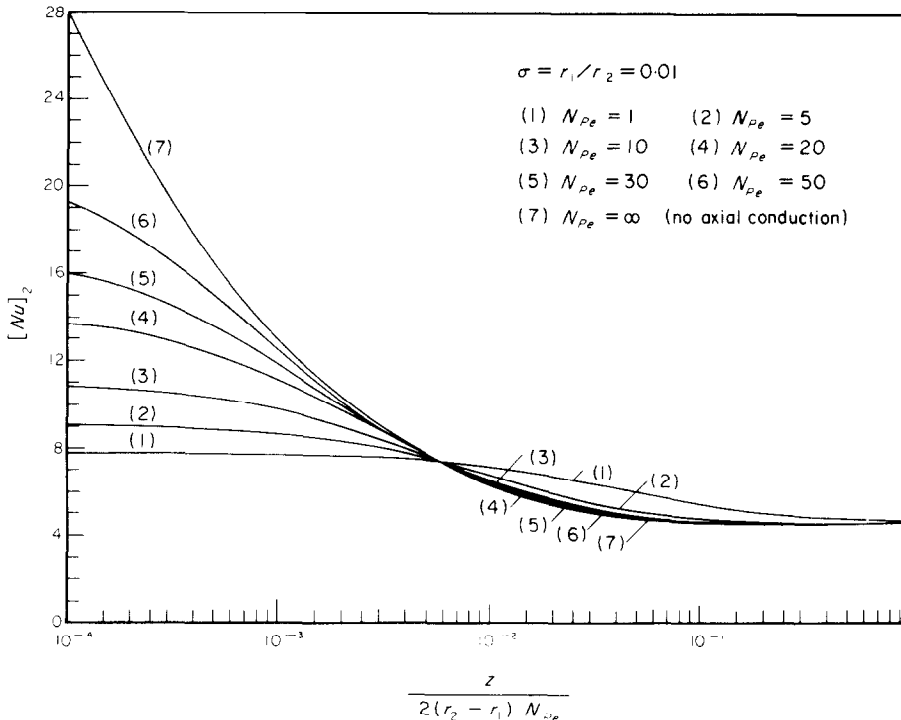


FIG. 2. Local Nusselt numbers  $[Nu]_2$  for  $\sigma = 0.01$ .

This proves the validity of the present solutions. By employing the computed eigenvalues and the associated constants, the local Nusselt numbers,  $[Nu]_1$  and  $[Nu]_2$ , were calculated from equations (41) and (42) for various Péclet numbers. The Nusselt curves thus obtained are shown in Figs. 2-7, for annuli having  $\sigma$  values of 0.01, 0.1, 0.3, 0.5, 0.7 and 0.9. As pointed out previously,  $N_{pe} = \infty$  corresponds to the limiting case of no axial conduction. It is worthwhile, therefore, to compare the results for this particular case with those reported by Lundberg *et al.* [4], who analyzed the corresponding problem on the assumption of negligible axial conduction. In [4], only the first few eigenvalues and the related constants are reported for several values of  $\sigma$ ; they were compared with those obtained in this study for  $N_{pe} = \infty$ , and excellent agreement was obtained. The local Nusselt numbers reported for  $\sigma = 0.1$  and  $\sigma = 0.5$  in [4] also agree very well with those obtained in this analysis.

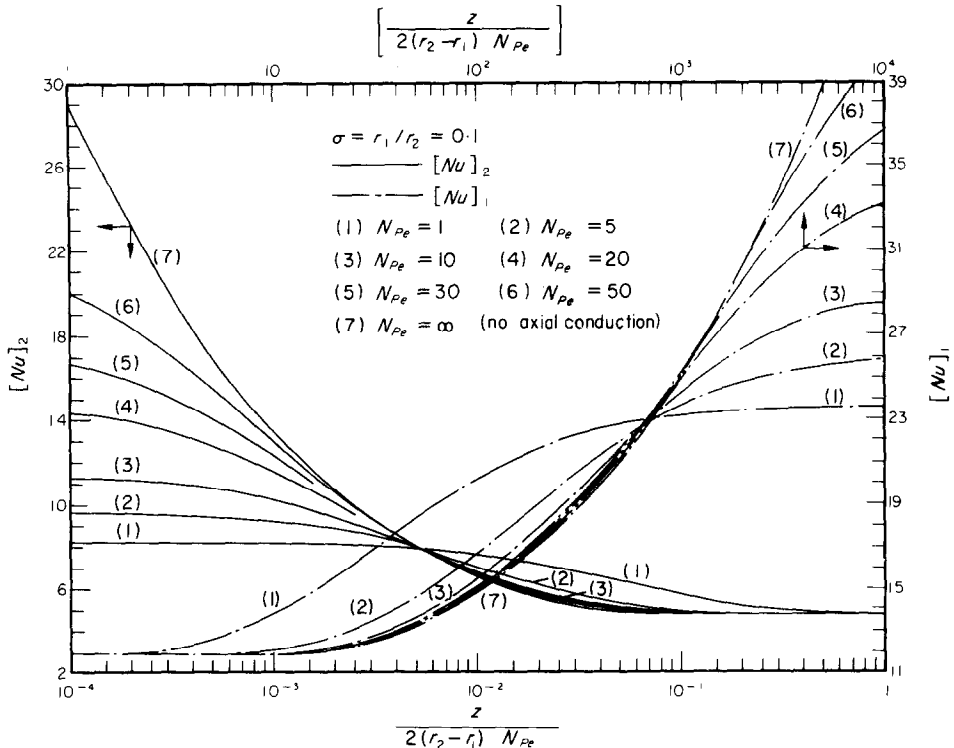


FIG. 3. Local Nusselt numbers  $[Nu]_1$  and  $[Nu]_2$  for  $\sigma = 0.1$ .

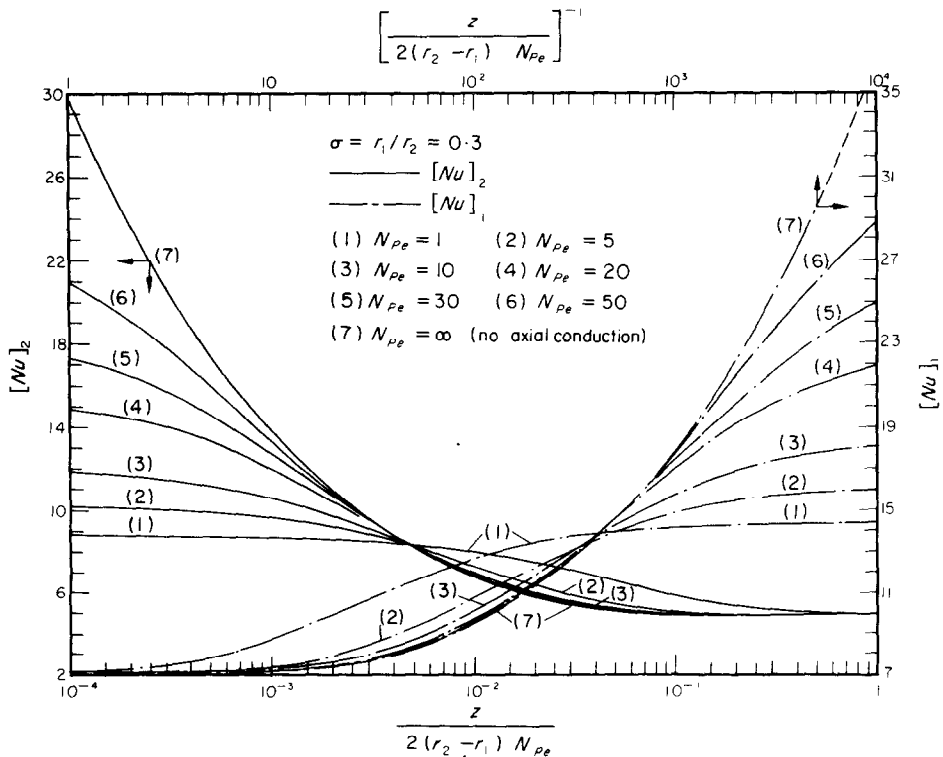


FIG. 4. Local Nusselt numbers  $[Nu]_1$  and  $[Nu]_2$  for  $\sigma = 0.3$ .

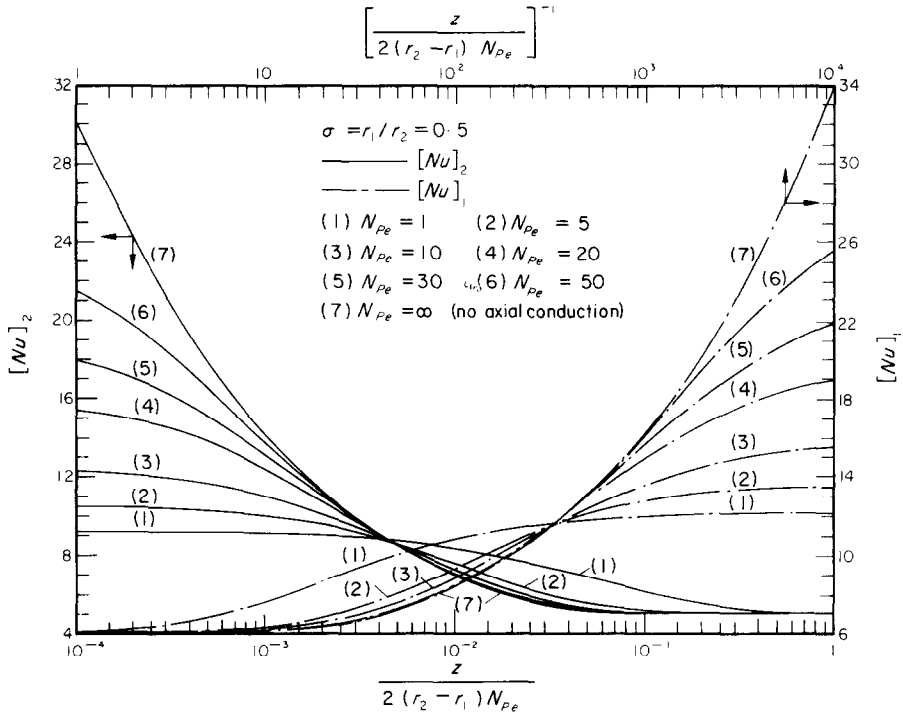


FIG. 5. Local Nusselt numbers  $[Nu]_1$ , and  $[Nu]_2$  for  $\sigma = 0.5$ .

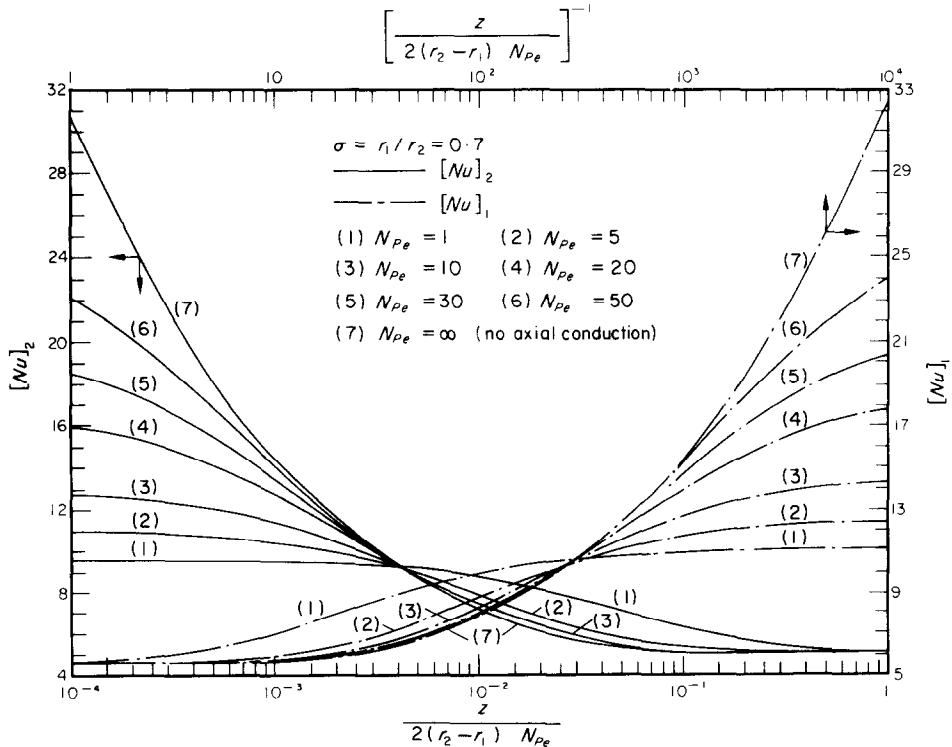


FIG. 6. Local Nusselt numbers  $[Nu]_1$ , and  $[Nu]_2$  for  $\sigma = 0.7$ .

From Figs. 2-7, it can be observed that, as  $N_{Pe}$  is reduced to below 100, both  $[Nu]_1$  and  $[Nu]_2$  tend to decrease at  $\eta \cong 0$  and become more uniform throughout the thermal-entry region. The Nusselt curves for various Péclet numbers, however, cross each other and reverse their orders of magnitude before reaching the fully developed values. This tendency is exactly identical to that found

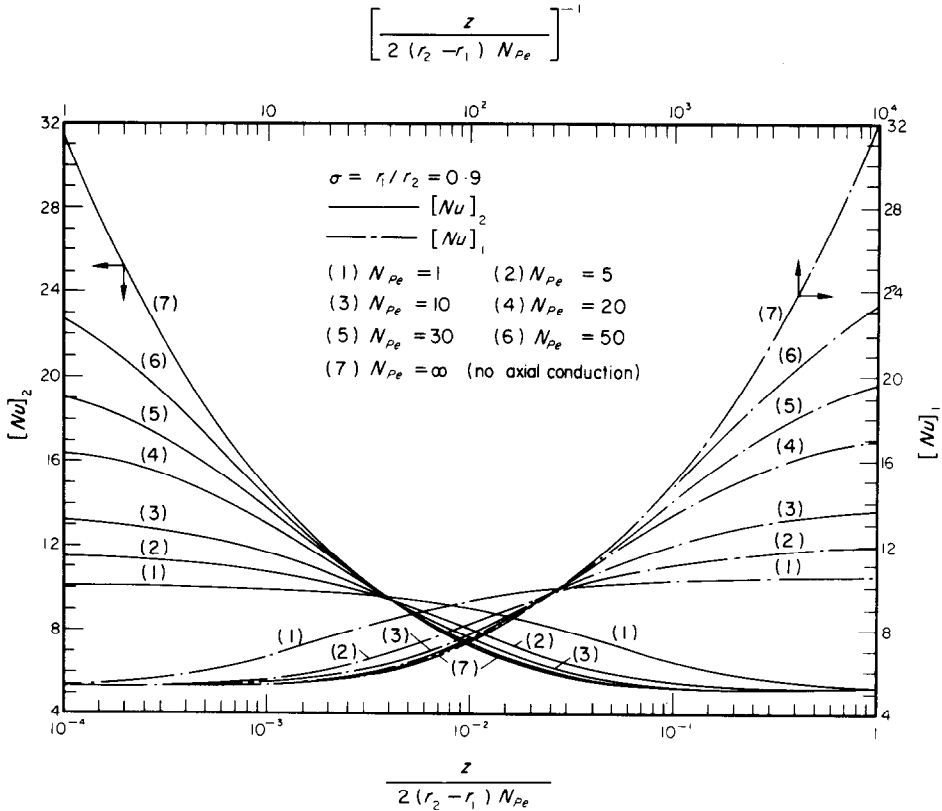


FIG. 7. Local Nusselt numbers  $[Nu]_1$ , and  $[Nu]_2$  for  $\sigma = 0.9$ .

in the previous study [2] for pipe and parallel-plate channel flows. It can also be noted that, for a fixed value of  $\sigma$ ,  $[Nu]_1$  is larger than the corresponding  $[Nu]_2$  in general. The two kinds of Nusselt numbers, nevertheless approach each other as  $\sigma \rightarrow 1$ , which corresponds to the limiting case of parallel plates. On the other hand, as  $\sigma \rightarrow 0$ ,  $[Nu]_2$  should reduce to those for the case of pipe flow. The  $[Nu]_2$  curves shown in Fig. 2 for  $\sigma = 0.01$  clearly exhibit this trend by comparison with the results obtained for pipe flow in the previous study [2].

Figures 8 and 9 illustrate respectively the variation of local fluid temperature profiles for the cases of  $j = 1$  and  $j = 2$ . These results, which are shown for  $\sigma = 0.5$  and for  $N_{Pe} = 1$  and  $N_{Pe} = 50$ , were obtained from equations (34)–(37). In the adiabatic region, the fluid temperature is seen to be uniform at sufficiently large negative value of  $\eta$ . For the case of  $N_{Pe} = 50$ , for which the effect of axial conduction is relatively small, this uniformity is roughly maintained throughout the adiabatic region. Even at  $\eta = 0$ , where the step jump in wall heat flux occurs, the fluid temperature is approximately uniform except the region close to the heated wall. As soon as  $\eta$  becomes positive,

the fluid temperature profile undergoes rather rapid change because of the imposed heat flux at the wall, causing a comparatively abrupt decrease of local Nusselt numbers. That this is not the case for  $N_{Pe} = 1$  is obvious. Because the heat conducted upstream into the adiabatic region is significant, a certain radial temperature profile is already established before the fluid reaches the point  $\eta = 0$ .

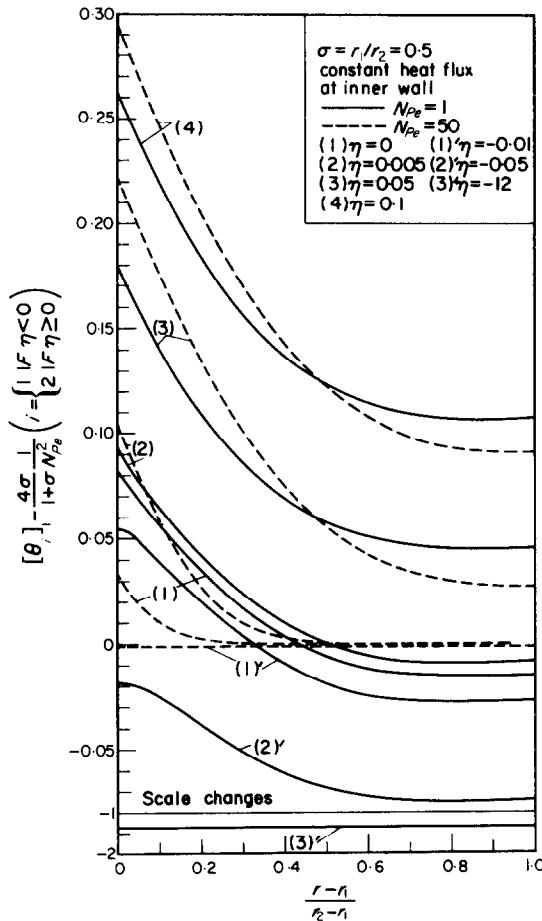


FIG. 8. Local fluid temperatures for the case where step jump in heat flux occurs at the inner wall.

In fact, it can be seen that the fluid temperature at  $\eta = 0$  deviates very significantly from uniformity, causing the temperature profile at  $\eta = 0$  to become nearly parabolic in shape. Such deviation appears to be larger if the step jump in heat flux occurs at the inner wall. Because of this, the temperature profile only changes slightly as the fluid flows through the heated region. This is the main reason why the local Nusselt number remains fairly uniform throughout the thermal-entry region if the Péclet number is small. In analyzing the effect of axial conduction in channel flow, therefore, it is incorrect to assume a uniform temperature profile at  $\eta = 0$ . Instead, the fluid temperature should be taken to be uniform at  $\eta = -\infty$ , as was done in this study.



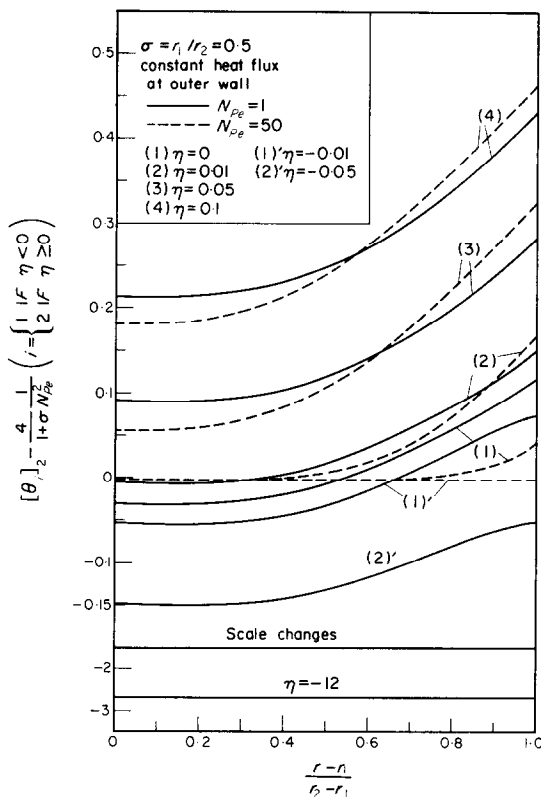


FIG. 9. Local fluid temperatures for the case where step jump in heat flux occurs at the outer wall.

REFERENCES

1. D. K. HENNECKE, *Wärme- und Stoffübertragung* 1, 177 (1968).
2. C. -J. HSU, An exact analysis of low Péclet number thermal-entry-region heat transfer in transversely nonuniform velocity fields. To be published in *A.I.Ch.E. Jl.*
3. I. P. NATANSON, *Theory of Functions of a Real Variable* (Transl. by L. F. BORON), Vol. 1, p. 195, Rev. Edn. Frederick Ungar, New York (1961).
4. R. E. LUNDBERG, P. A. MCCUEN and W. C. REYNOLDS, *Int. J. Heat Mass Transfer* 6, 495 (1963).

SOLUTIONS THÉORIQUES CORRESPONDANT AU TRANSFERT THERMIQUE POUR LES NOMBRES DE PECLÉT FAIBLES DANS LA RÉGION D'ENTRÉE POUR UN ÉCOULEMENT LAMINAIRE À L'INTÉRIEUR D'UN ESPACE ANNULAIRE

**Résumé**—On obtient les solutions exactes de température et les courbes théoriques de Nusselt, valables pour les nombres de Péclet variant depuis un jusqu'à l'infini concernant le transfert de chaleur dans une région d'entrée pour un écoulement laminaire à travers un espace annulaire, soumis à un échelon de flux de chaleur à la paroi pour  $z = 0$ . Pour tenir compte de l'effet de conduction axiale qui est important pour des nombres de Péclet faibles, la température du fluide à l'entrée est choisie uniforme pour  $z = -\infty$  et les vingt premières constantes sont calculées séparément pour la région adiabatique ( $-\infty < z \leq 0$ ) et la région chauffée ( $0 \leq z < \infty$ ).

En construisant deux ensembles de fonctions orthonormées provenant des fonctions propres non orthogonales, les coefficients des développements en série sont alors déterminés de façon que les températures les gradients longitudinaux de température pour les deux régions coïncident pour  $z = 0$ . Les solutions

de température correspondant au cas limite  $N_{pe} = \infty$  montre l'excellent accord avec celles publiées par Lundberg *et al.* [4], qui analysèrent le problème de la région d'entrée en négligeant la conduction axiale.

#### THEORETISCHE LÖSUNGEN FÜR DEN WÄRMEÜBERGANG BEI KLEINER PÉCLÉT-ZAHL IM EINLAUFGEBIET LAMINAR DURCHSTRÖMTER KONZENTRISCHER RINGRÄUME

**Zusammenfassung**— Für das thermische Einlaufgebiet bei laminarer Strömung durch einen konzentrischen Ringkanal werden exakte Lösungen der Temperatur und des theoretischen Verlaufs der Nusseltzahlen angegeben. Die Lösungen gelten für Péclet-Zahlen von 1 bis  $\infty$  und unter der Bedingung einer stufenförmigen Änderung der Wärmestromdichte der Wand bei  $z = 0$ . Um den Einfluss der axialen Wärmeleitung zu berücksichtigen, der bei kleinen Péclet-Zahlen bedeutend ist, wurde die Eintrittstemperatur des Fluids als konstant angenommen bei  $z = -\infty$ . Die ersten zwanzig Eigenwerte für das adiabate Gebiet ( $-\infty < z \leq 0$ ) und das beheizte Gebiet ( $0 \leq z < \infty$ ) wurden getrennt berechnet. Durch die Konstruktion zweier Scharen orthonormaler Funktionen aus den nichtorthogonalen Eigenfunktionen wurden die Serienexpansionskoeffizienten so bestimmt, dass sowohl die Temperaturen als auch die axialen Temperaturgradienten der beiden Gebiete bei  $z = 0$  übereinstimmten. Die Lösungen für die Temperatur bei der Grenzbedingung  $Pe = \infty$  stimmen sehr gut überein mit denen von Lundberg *et al.* (4), die das Problem des Einlaufes unter Vernachlässigung der axialen Leitung untersuchten.

#### ТЕОРЕТИЧЕСКОЕ ИССЛЕДОВАНИЕ ТЕПЛООБМЕНА В ЛАМИНАРНОМ ТЕЧЕНИИ В КОНЦЕНТРИЧЕСКИХ ЗАЗОРАХ ПРИ НИЗКИХ ЧИСЛАХ ПЕКЛЕ ВО ВХОДНОМ ТЕПЛОВОМ УЧАСТКЕ

**Аннотация**— Для входного теплового участка при теплообмене в ламинарном течении через концентрический зазор получены точные решения для температуры и расчетные кривые чисел Нуссельта, справедливые для чисел Пекле от 1 до  $\infty$ , для скачка теплового потока на стенке при  $z = 0$ . Для учета осевой теплопроводности, имеющей значение при низких числах Пекле, температура жидкости на входе считается постоянной при  $z = -\infty$ . Рассчитаны первые двадцать собственных значений в отдельности для адиабатической области ( $-\infty < z < 0$ ) и для области нагрева ( $0 < z < \infty$ ). Затем путем построения двух систем ортогональных функций из неортогональных собственных функций определялись коэффициенты разложения, так что как температуры, так и градиенты температур для двух областей согласовались при  $z = 0$ . Решения температуры, соответствующие предельному случаю  $N_{pe} = \infty$  прекрасно согласуются с данными, опубликованными Лундбергом, Мак-Гуеном и Рейнольдсом (4), которые получили аналитическое решение для входной области в пренебрежении аксиальной теплопроводности.